SACS2 Status Report by GECO
January 2002 – version 0.1

Document Contact

Trygve Randen
Schlumberger Stavanger Research
Risabergveien 3, Tananger
P.O. Box 8013
4068 Stavanger
Norway
Tel.: +47 51 94 64 71
Mob.: +47 402 47 478
E-mail: trygve.randen@slb.com

Authors

Hilde Grude Borgos
Geir Vaaland Dahl
Kristine Årland Halvorsen
Terje Iversen
Magne Lygren
Trygve Randen
Thorleif Skov

WP 8-11 – Geophysical Interpretation   lead by GECO

As previously concluded from the geophysical community of the SACS2 project, seismic data is very well suited to mapping the presence and distribution of the injected gas in the sub-surface. The CO_2 acts as a very good "contrast agent" for the seismic signal. However, questions still to be answered are: Can we make account for all the injected gas (with high confidence) and can we, from the seismic data, explain the migration path of the gas? The latter question has turned out to be very important in order to integrate seismic time lapse measurements with the reservoir model.

Several attempts are being taken to answer these questions and will be reported in the subsequent sections. First, the gas is most likely constrained in its vertical movement by thin shale layers within the Utsira sand. Furthermore, migration to the overlying sand wedge is observed. The migration appears to be under spill points not *obvious* from the baseline seismic survey. Two hypotheses are examined, either that the gas seepage is governed by faults and/or that it is governed by local thinning of the shale layers. The latter question can probably only be answered by examination of the top Utsira formation, as the intra-Utsira shales are not very clearly imaged on the baseline survey.

Next, making account for the injected gas is a very complex task, with large uncertainties. In this document, we report on several approaches to estimate the gas present according to the time-lapse seismic data. First we attempt to make a geometric estimate of the gas volume present by a method called "umbrella closure". Another attempt is then made using a probabilistic approach to top and base gas cloud detection. Next we attempt to couple the reservoir simulator with the measured seismic through creation of synthetic seismic data from the model, and tune the parameters until we converge towards a match. Finally, we are pursuing two different approaches towards differential impedance estimation, one based on pre-stack analysis and one based on post-stack inversion. The effort on the case study has been significantly increased over the last few months.

As already mentioned, the SACS2 project has clearly revealed the value of seismic data for monitoring the CO_2. However, if rolled out on a wide range, not every re-injection project can enjoy the immense effort of a pilot study. Hence it will be of significant importance to develop an efficient workflow for the data analysis. One element here is the "best practice manual". However, also efficient tools will be necessary to ensure the efficiency. Consequently a significant research and technology development (RTD) effort is being devoted to the development of efficient tools for the purpose. A status report on this RTD element is also reported.

It is noted that this report is an interim report and some of the work tasks do require more effort to draw proper conclusions.

Mapping of faults with possible influence on gas migration

Faults in the Utsira formation can potentially control (or at least affect) the horizontal distribution of the injected gas, if they represent permeability barriers for horizontal flow. Faults can also be potential leaking points for vertical flow through displaced or damaged thin impermeable layers, like shale.

Leakage of gas from the Utsira formation, into the overlying sand wedge layer has been observed on the time-lapse seismic data from 1999. Continued leakage is observed from the 2001 data. The explanation of this leakage can be faults that cut through the Utsira formation and act as leakage points due to displacement of the intermediate clay layer (**Figure 2**, **Figure 3**, and **Figure 4**).

Only the 1994 base-line survey has been used for the fault interpretation. Because of the poor data quality, and the fact that potential faults at this depth interval have displacement values close to the limit of vertical seismic resolution, makes manual interpretation difficult. Automatic fault extraction with a new, patent pending software tool is therefore used in addition to manual interpretation. The new fault-tracking tool is efficient to indicate and guide the fault interpretation in seismic of poor quality (**Figure 5**). An associated navigation tool is used for further filtering of faults from other features. Surface attributes like amplitude maps and layer-thickness maps together with a resolution-enhanced cube is utilised for the manual interpretation.

So far, four normal faults with displacement close to the vertical resolution limit have been interpreted in the gas-cloud area (**Figure 1**, **Figure 2**, **Figure 3**, **Figure 4**, and **Figure 6**). Faults A and B dip to the south, C and D dip to the southeast (**Figure 2**, **Figure 3**, and **Figure 4**). All four faults are possible candidates for gas leakage from the Utsira formation to the Sand wedge layer (**Figure 2**, **Figure 3**, **Figure 4**, and **Figure 6**). The faults are either positioned in the leaked gas zones or are defining the edge of them in both the 1999 and the 2001 time-lapse seismic. In addition to act as a leakage point, fault D seems to define the edge of the gas distribution in the deeper part of Utsira formation. This is only true in parts of the gas-cloud area.

None of the reflections in the gas-cloud area show clear terminations or separation that is clearly due to fault movement. Small apparent reflection-terminations and separations can be seen in a great number, but are more probably due to other features. It is therefore difficult to isolate the true faults. Only surfaces with a certain vertical and horizontal extent are believed to represent faults. Note that the gas affected time-lapse seismic was hidden away when the faults where interpreted, and had no influence on the result.
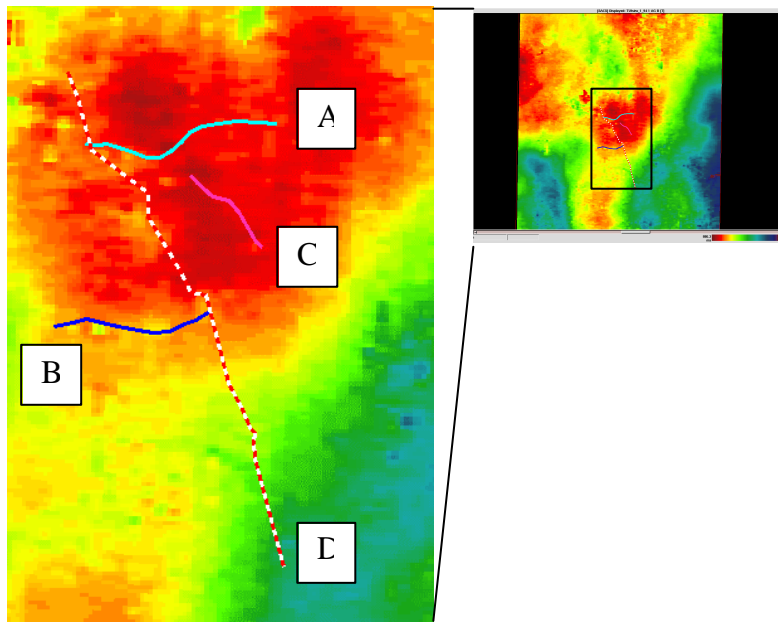

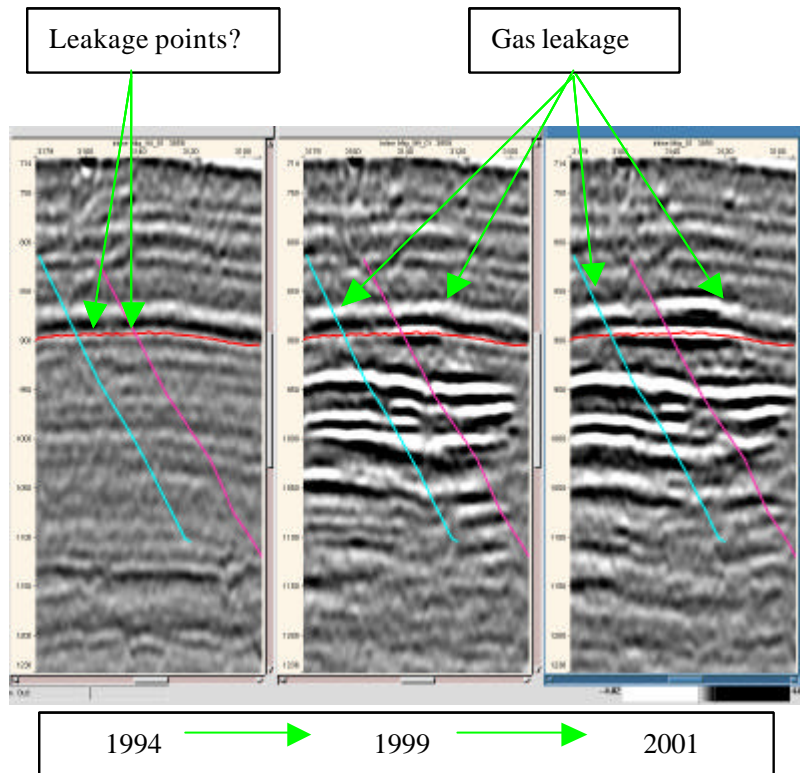**Figure 1 Fault boundaries of faults A, B, C and D on the Top Utsira horizon.**

Figure 2 Faults C and A represent possible leakage points where they cut Top Utsira. The Top Utsira horizon is marked with red.
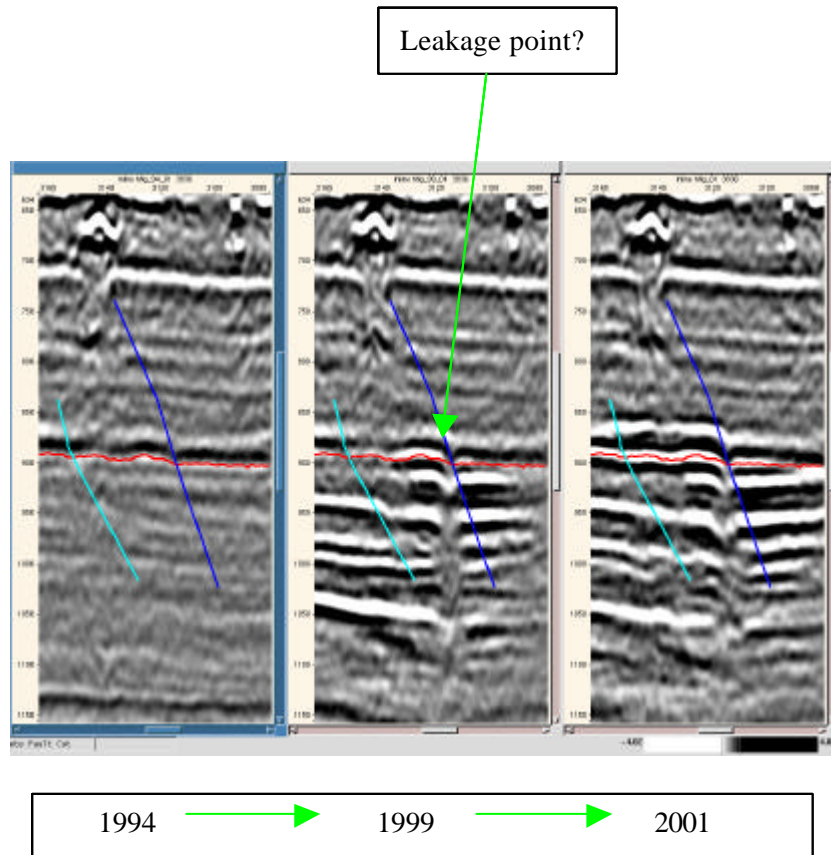

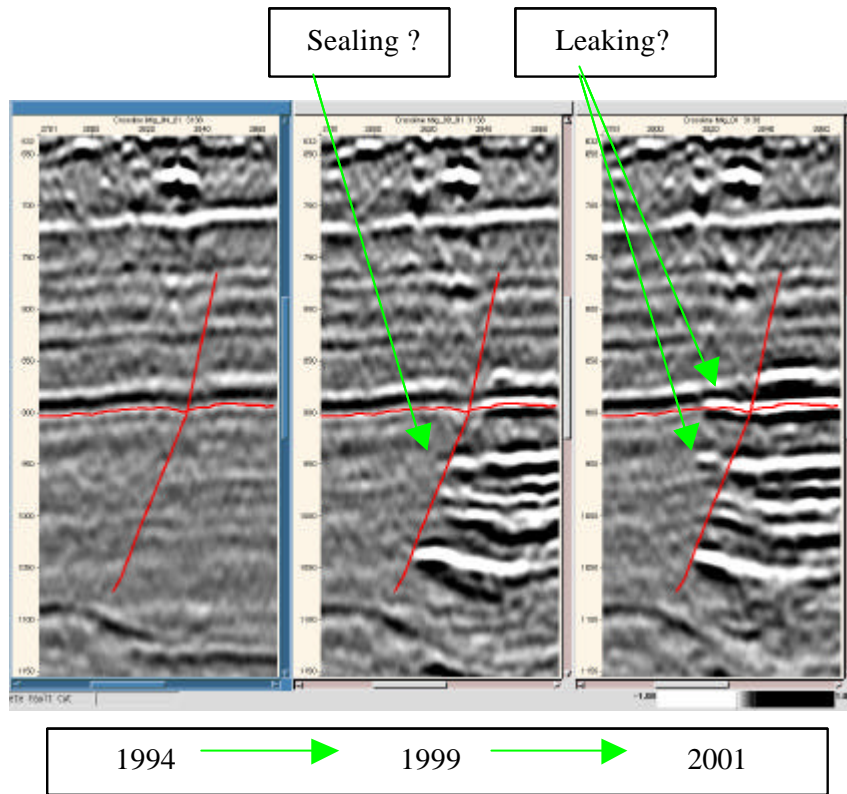**Figure 3 Fault A and B. Fault B represents a possible leakage point.**

Figure 4 Fault D represents a possible flow barrier for the gas in the deeper part of Utsira formation. It is also a possible leakage point through the Top Utsira layer boundary.
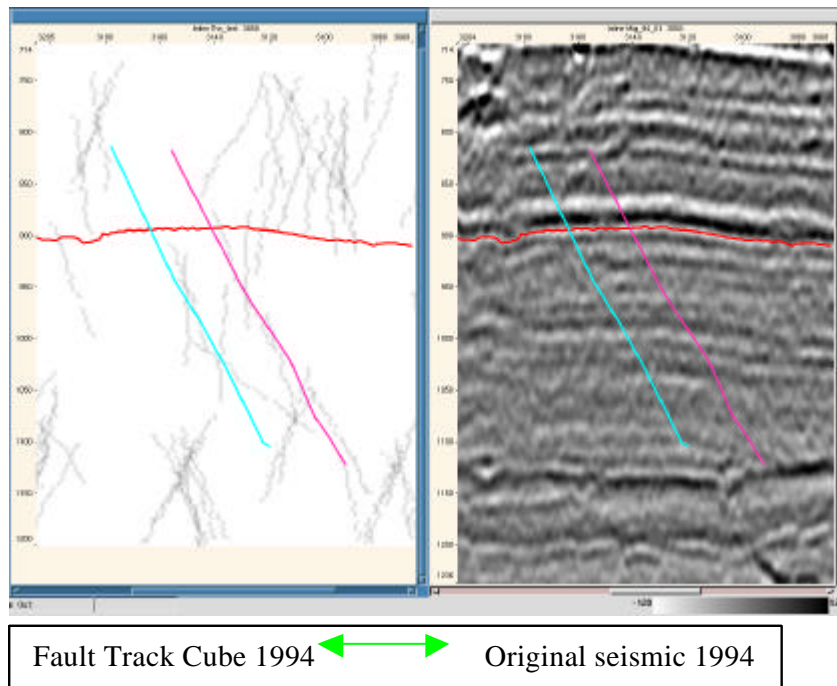

Figure 5 New attribute cubes are used for guiding the manual fault interpretation. Faults A and C are displayed.
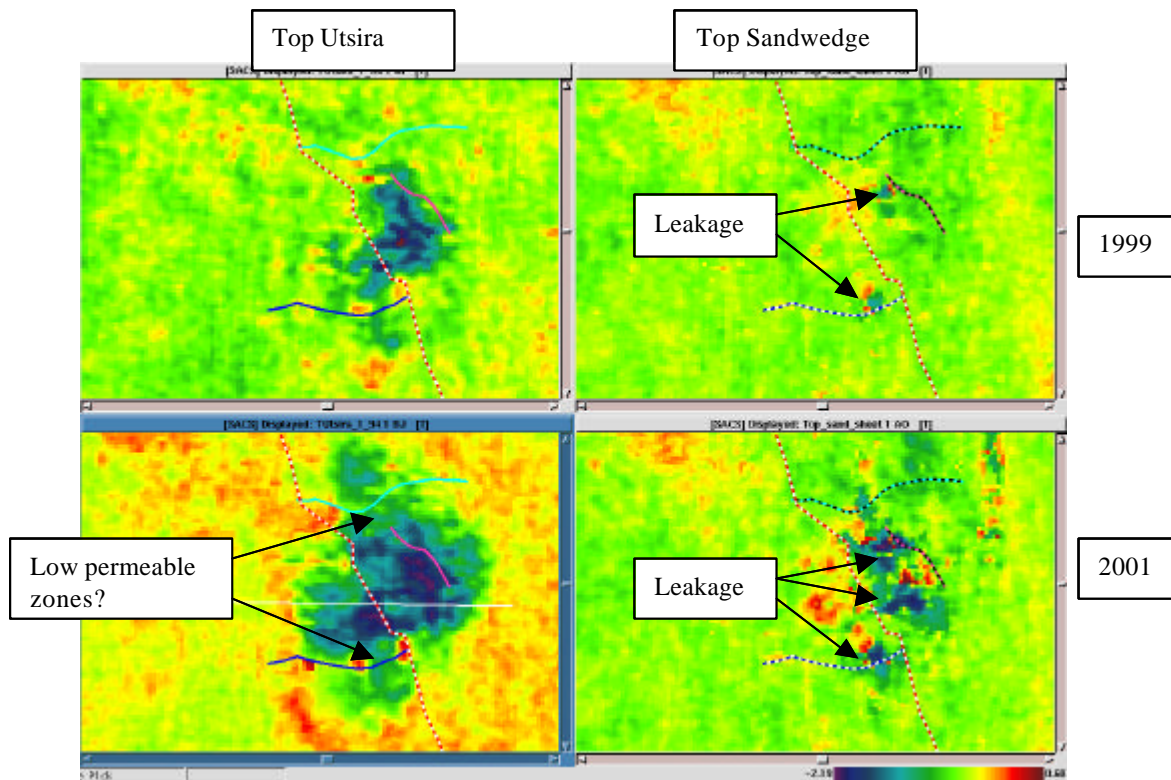
Figure 6 Maps showing instantaneous amplitude along the Top Utsira formation (left) and Top sand wedge (right). Faults A and B act as possible low permeable zones along the Top Utsira layer boundary. All four faults may influence leakage into and distribution of the gas.

Shale seal quality estimation by Super Resolution mapping

Super Resolution mapping has been applied to study the thickness of the sealing shale layer above the Utsira formation, to investigate possible leakage zones in the shale. The baseline data (Mig_94 and Mig_94_01, respectively the 1999 and 2001 re-processed versions of the baseline-survey) is used. The thickness of the shale layer and the sand wedge above is small, resulting in tuning effects in the seismic signal. The Super Resolution algorithm is constructed to deal with tuning problems, and aims at deconvolving the interference in the seismic signal. The deconvolution is performed assuming the number of reflectors and the wavelet is known. The wavelet is extracted using our patent pending 3D blind deconvolution (3DBD).

The top of the Utsira formation is interpreted on a negative event on the seismic cube, and the top of the sand wedge as the next negative event above top Utsira. The positive event in between is assumed to be the result of interference between these two reflectors and the base of the sand wedge. Super Resolution mapping is used to determine the exact position of the base of the sand wedge in the tuning region, with the top of the sand wedge and the top of Utsira interpreted in advance.

The Super Resolution algorithm was first run on the 1999-re-processed version of the baseline seismic, Mig_94. **Figure 7** shows an inline section through the seismic cube, with the pre-interpreted reflectors and the interpretation obtained using Super Resolution. The result shows some variations in the shale layer thickness, with smaller regions where the shale layer is very thin. The algorithm was next run on the 2001-re-processed baseline data, Mig_94_01, in a region above the injection point: inlines 3751-3950, crosslines 3051-3300. **Figure 8** shows the interpretation in an inline section, **Figure 9**a shows the resulting thickness of the shale layer and **Figure 9**b the thickness of the sand wedge. For the new processed data the interpreted base of the sand wedge is smoother than on the original data, and the shale layer thickness

varies less. The shale layer thickness in **Figure 9**a shows some variations in thickness laterally, but for the Mig_94_01 seismic cube the interpretations do not reveal any obvious leakage points in the shale layer in the region where the leakage is observed on the time lapse data. The different results for the two different baseline seismic cubes may be a result of the noise level in the seismic data, or may be related to differences in the estimated wavelets for the two cubes.
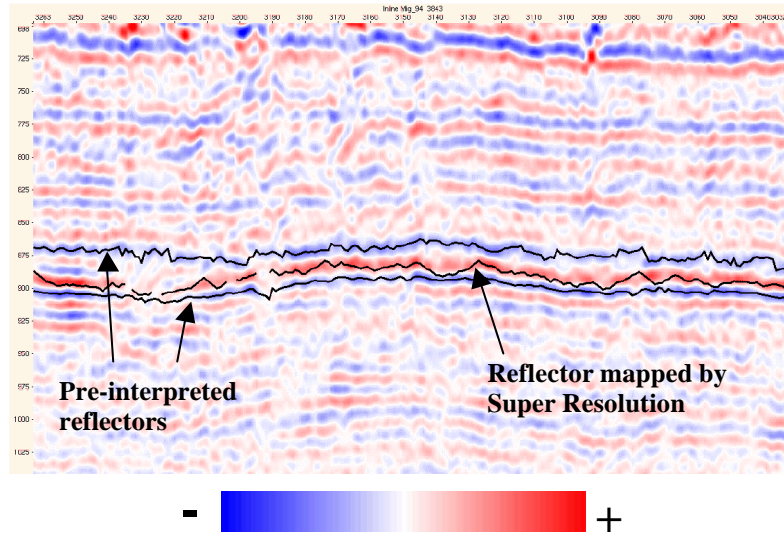

Figure 7 Seismic inline section (Mig_94) showing the Super Resolution mapping of the base of the sand wedge. The top and bottom reflectors are interpreted in advance, and are used as input to the algorithm.
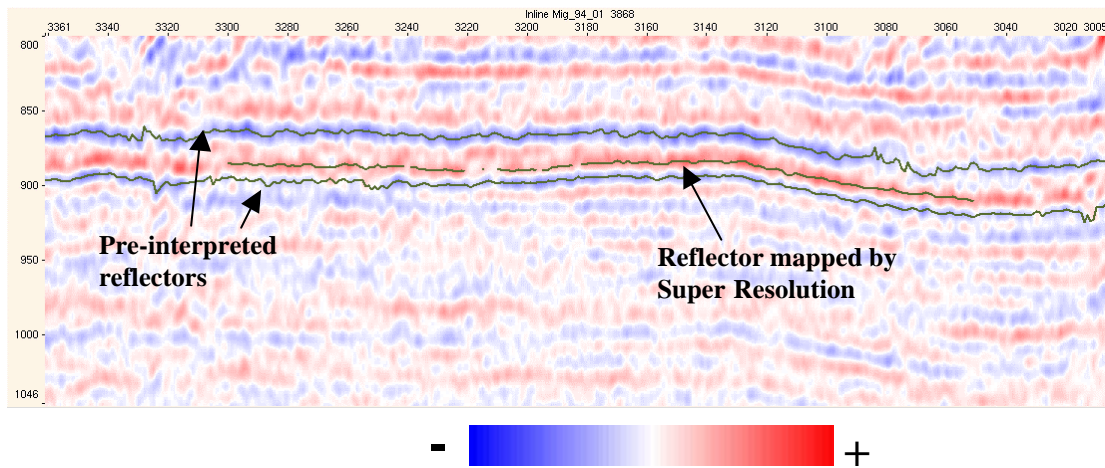

Figure 8 Seismic inline section (Mig_94_01) showing the Super Resolution mapping of the base of the sand wedge. The top and bottom reflectors are interpreted in advance, and are used as input to the algorithm.
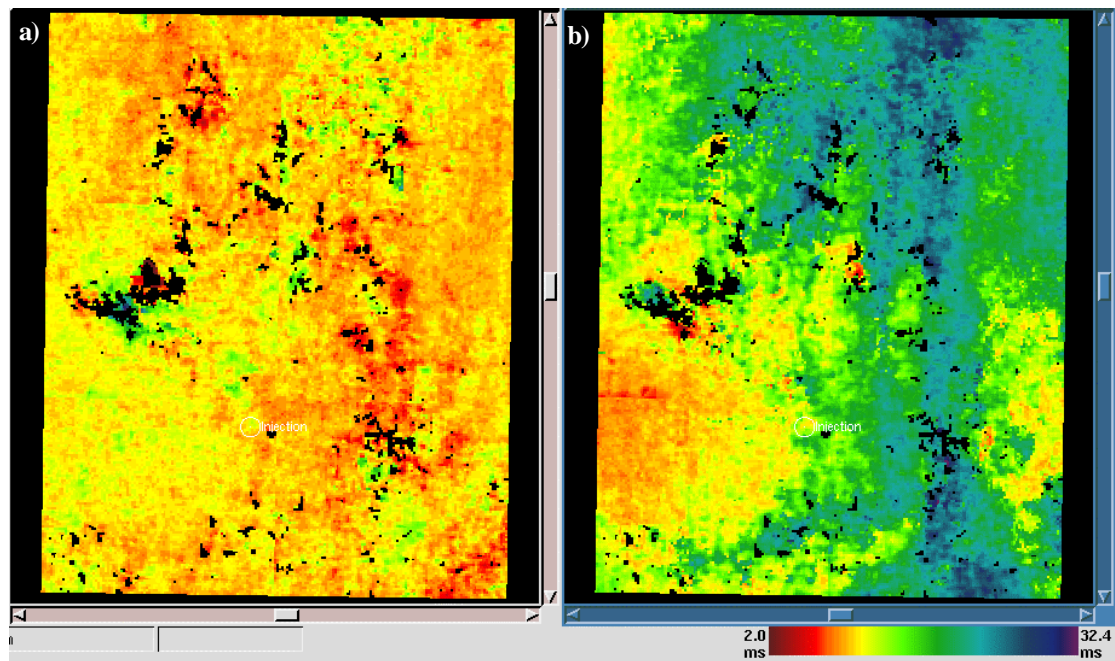
Figure 9 Thickness of a) shale layer and b) sand wedge on Mig_94_01.

Structurally derived gas volume estimation

The Utsira formation has a gentle dome structure in the area where the gas is situated. The internal reflections from the formation have low continuity and are therefore difficult to interpret. The horizontal distribution of the gas closely follows the dome structure, while the vertical distribution is anticipated to be captured in structurally defined pockets. If the sealing roofs of these pockets have more or less the same shape as Top Utsira and the bases are controlled by spill points on the flanks, the gas volume can be calculated by a software tool called Umbrella Closure.

The gas volume will be calculated in the nearest future. So far the structural model is under construction. Figure 7 and 8 shows the mapped gas clouds (or pockets) from the 1999 time-lapse seismic. The endpoints of these clouds are assumed to be positioned at the right time-level. A sealing roof that gives a close match to both the dome shape of Utsira formation and the endpoints will be placed over each of the clouds.

Estimation of relative interval velocity changes in the gas zones

The relative interval velocity changes in the gas zones have been estimated based on 3D post-stack travel-time interpretation of the 3 data sets available: 1994, 1999 and 2001[1]. The relative velocity changes are estimated by a procedure called Vertical Seismic Scaling (VSS)[2] that calculates the relative velocity changes from the time-lapse differences in travel-time within a layer bounded by two horizons. Detailed interpretations are required as input to the VSS procedure in order to obtain plausible estimates of the velocity changes. Moreover, it is expected that a higher velocity resolution is obtained if the Utsira layer is subdivided into thinner layers. Unfortunately, the signals are more or less discontinuous in and around the

---

[1] To ensure that all the data is processed by the same procedure the 1994 and 1999 data sets were re-processed simultaneously with the 2001 data.

[2] The VSS procedure is developed by Schlumberger Stavanger Research and is available in the GeoFrame 3.8 and 4.0 software packages.

zone of interest, and in order to interpret the number of layers required for a detailed velocity profile, advanced automated 3D travel time extraction procedures will be needed. In this work the interpretations are made manually with support from resolution-enhanced and extrema cubes created in GeoFrame™. As a starting point, we have therefore restricted our interpretations to the following horizons: Top, Mid and Base Utsira, as well as Hordaland.

So far we have been able to find detailed and consistent interpretations of Top and Base Utsira for all data sets (1994, 1999 and 2001). As the gas is mainly located below Top Utsira the interpretation of this horizon is the same for all data sets. An interpretation of Top Utsira is shown in figure 10. The Base Utsira interpretations can be seen in figure 11. Note the conformity in shape between Top Utsira in figure 10 and the gas distribution in figure 11. The relative P-velocity changes for the interval between Top and Base Utsira are shown in figure 12. We are currently working on the interpretations of Mid Utsira and Hordaland, and as soon as these interpretations are completed we will estimate the relative interval velocity changes for the sub-layers.

As indicated by the name of the VSS procedure, it also creates "scaled seismic" that can be used to assess the probability that the interpretations are plausible. The time-lapse seismic is stretched vertically according to the travel time difference between the time-lapse interpretation and a chosen reference interpretation. (In this case the interpretation made on the 1994 data is used as a reference interpretation as this data set was acquired before the gas injection commenced). If the stretched version of the time-lapse seismic is approximately equal to the reference seismic this may indicate that the time-lapse interpretation is reliable.
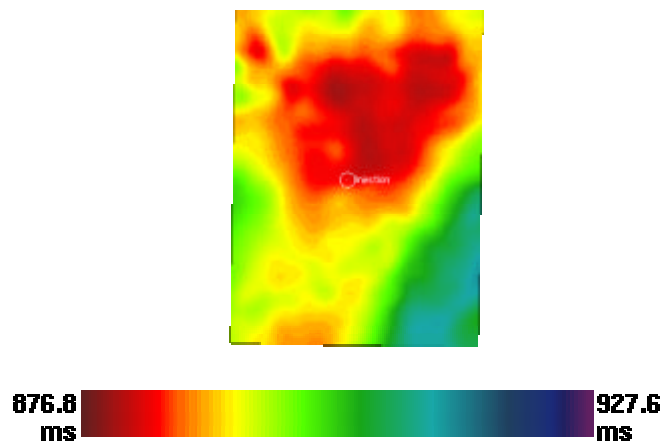

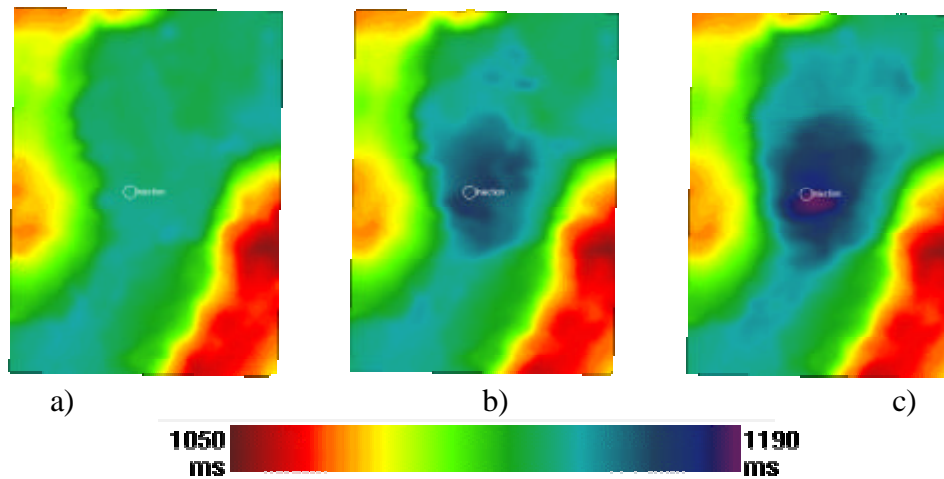**Figure 10 Interpretation of Top Utsira on the 1994 data.**

Figure 11 Interpretations of Base Utsira on the a) 1994 data, b) 1999 data and c) 2001 data. The injection point is indicated in the middle of each figure. The travel time is indicated by the colourscale above.
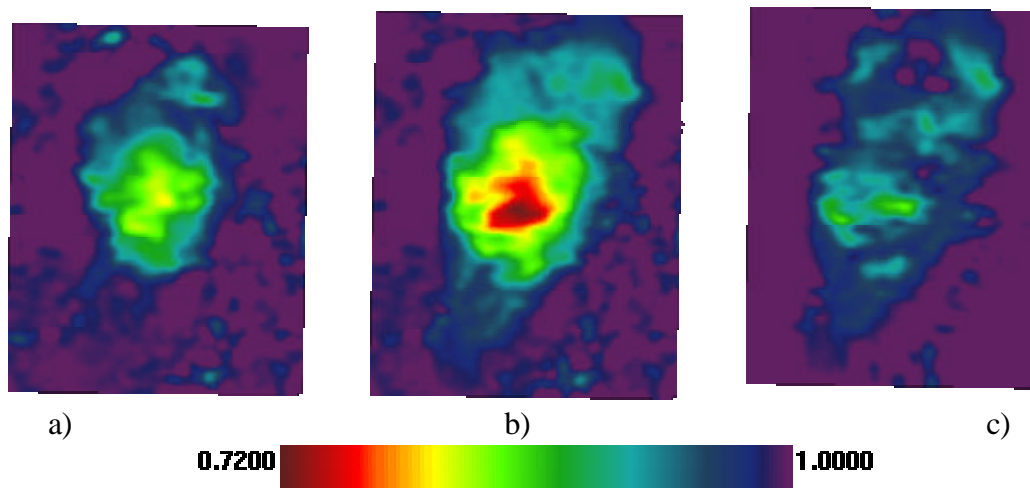

Figure 12 Relative P-velocity changes in the interval between Top and Base Utsira a) from 1994 to 1999, b) from 1994 to 2001 and c) from 1999 to 2001. The relative velocity changes are indicated by the colourscale above.

4D amplitude inversion (Estimation of relative impedance changes)

We have made an effort to quantify the time-lapse reflectivity changes in the gas zone by a two-step procedure. First, 4D Blind Deconvolution (4DBD) is applied to two different seismic cubes (the 1994 cube and either of the time-lapse cubes, for instance). The 4DBD routine assumes that the reflectivity is constant and outputs an estimate of a common reflectivity cube for the two input cubes. One wavelet cube and one global wavelet are also estimated for each cube. Next, the reflectivity and wavelet cubes for one of the seismic input cubes are used as input to a 3D deconvolution routine that estimates a reflectivity cube as well as another wavelet cube and global wavelet for the seismic input cube. The same is done for the second seismic input cube, for which a corresponding reflectivity cube, wavelet cube and global wavelet estimate are obtained.

The reflectivity cubes provide a valuable attribute input to the simulator flow-model, and in the next step we will study the flow-model simulations with these cubes as input. The 4DBD wavelet cubes will also be used to assess the repeatability of the seismic survey.

Furthermore, we are planning to estimate the time-lapse impedance chances in the gas zone, and there are several ways in which this can be done. Unfortunately, significant uncertainties related to some major gas parameters introduce complications to some of the procedures that could be used. We have therefore decided to start out with the Best Feasible Approximation (BFA) module that is available in the Charm module in AMain, Charisma/GeoFrame™.

The BFA module requires an initial geological impedance model as input and outputs the best approximation to this model, within a range defined by some given constrains. The initial model is based on well log information as well as a surface model containing the structural layers in the geometrical model. In our case we will start out with a surface model containing the Top and Base Utsira horizons. The acoustic impedance logs in and around the SACS survey area are interpolated and included in the model as initial impedance estimates. (As there are few well logs available, it might be useful to somehow add the velocity profile to the input information). By use of this initial model, as well as the seismic data and the wavelet obtained from the 4DBD run, the BFA routine iterates until it finds the "best feasible approximation" to the initial model.
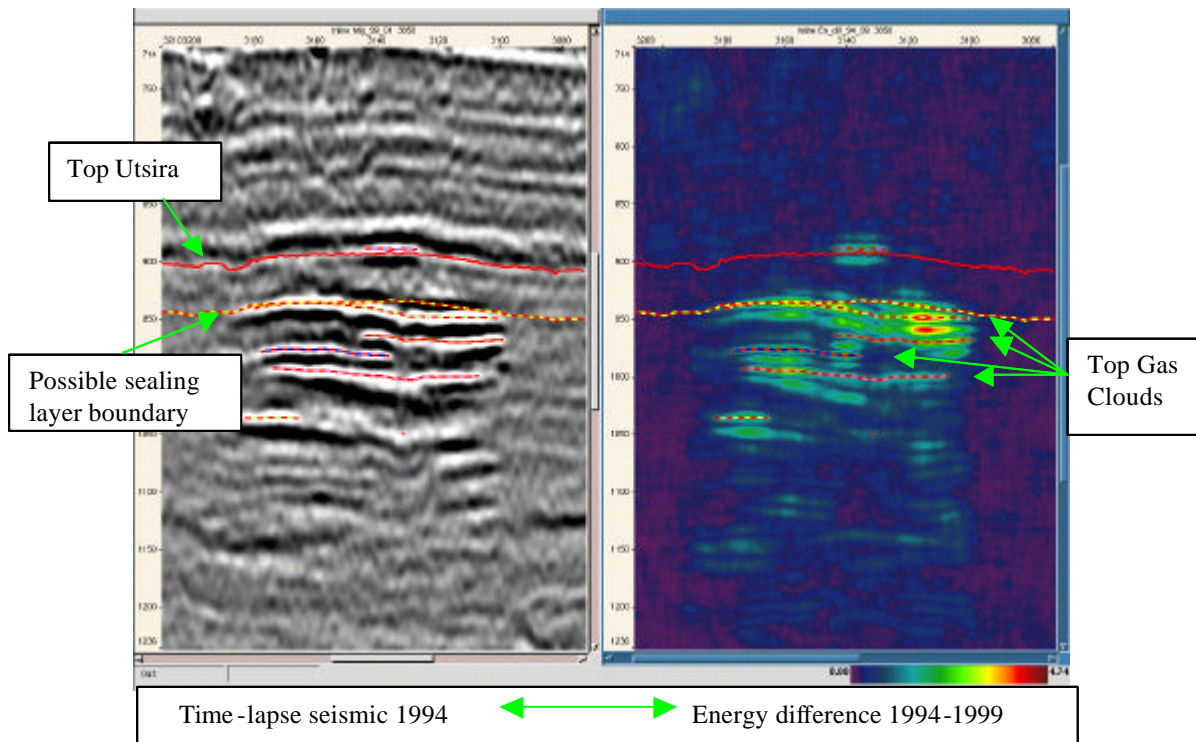

Figure 13 The endpoints of the mapped gas clouds will be used to adjust the sealing layer to the right depth level.
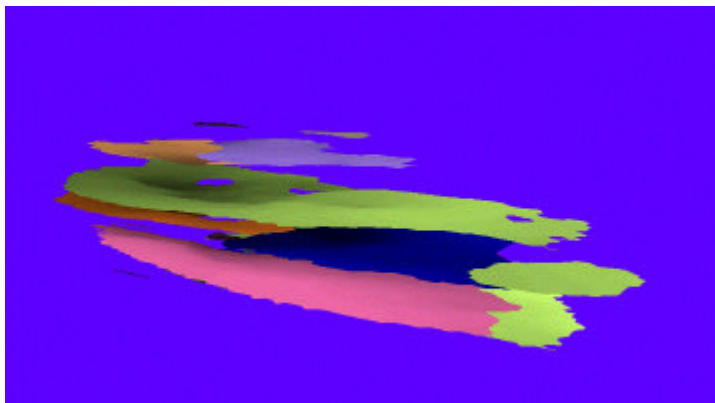
Figure 14 Top Gas Clouds.

Top and base gas pocket detection by Super Resolution mapping

For thin layers of gas, the reflection from the top and base of the gas pocket will result in interference in the seismic signal. Super Resolution mapping is applied, trying to map the vertical extent of some of the gas pockets. The first time-lapse data (Mig_99_01) is used. Reflectivity estimates obtained from 3DBD are studied prior to running the Super Resolution algorithm. The 3DBD results reveal which seismic maxima and minima are actual reflectors and which are more likely to be side lobes. These results indicate in which regions Super Resolution should be used to continuously map the top and base of the gas pockets.

Figure 15 shows an inline section through the reflectivity cube estimated using 3DBD. Reflectors from gas pockets should appear as pairs of reflectors, negative above positive. Some potential reflectors from gas pockets are interpreted from the reflectivity cube in **Figure** 15, and Super Resolution mapping is run in these regions. The results are shown in **Figure** 16, illustrated on an inline section from the seismic cube Mig_99_01. The thickness of each gas pocket is illustrated in **Figure** 16. The mapped gas clouds show clear tendencies of being thinned towards the rim of the clouds, as we would expect from a dome-geometrically confined gas pocket.
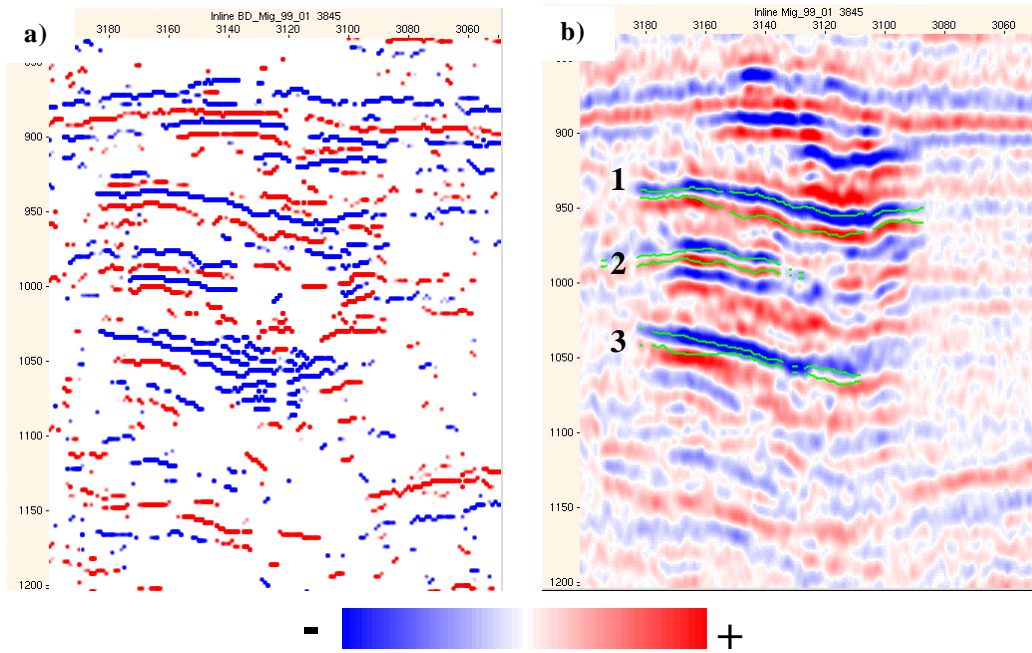
Figure 15 a) shows the reflectivity cube estimated by 3DBD and b) shows the seismic data (Mig_99_01) with the results from Super Resolution mapping of some of the gas pockets.
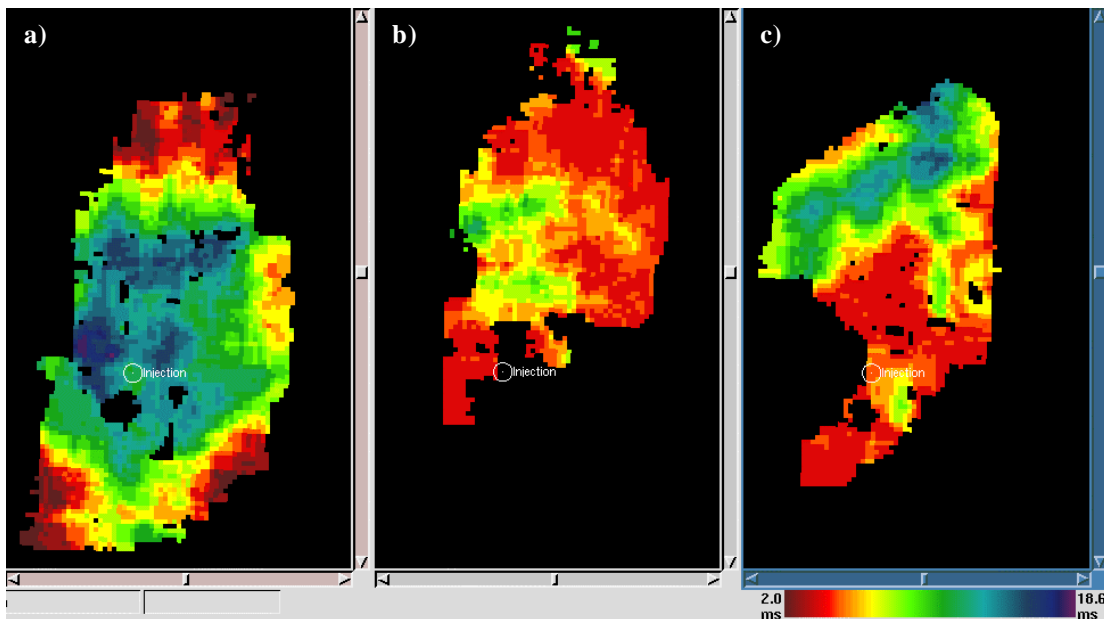

Figure 16 Thickness of gas pockets found by Super Resolution. The gas pockets in a), b) and c) corresponds to the gas pockets marked 1, 2 and 3 in Figure b respectively.

The Super Resolution algorithm is instructed to map two reflectors throughout a defined region of interest. In some regions, especially in **Figure** 16 and **Figure** 17, the resulting reflectors lies at a constant short distance of 2-4ms, related to a minimum allowed distance used in the algorithm. In these regions the results from Super Resolution are somewhat unreliable, indicating that the algorithm is not able to detect two well-defined, sufficiently separated reflectors. Note that the physical explanation can be either that the reflectors are very close or that there is no base gas reflector in the examined interval. Another test of the existence of a base gas reflector corresponding to a large difference in gas saturation (keeping the non-linear nature of the impedance with respect to gas saturation, to some extent illustrated in **Figure** 17, in mind) is obtained

by examining the amplitude of the identified potential base gas reflectivity, **Figure** 17. A reliable estimate of a large saturation difference will yield a large reflectivity. Low estimated reflectivity thus corresponds to either a small saturation difference or a low reliability estimate.
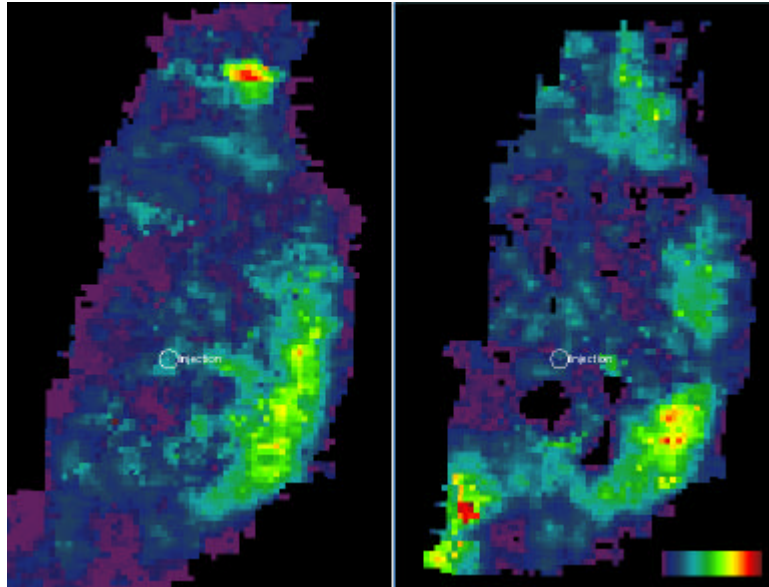

Figure 17 Magnitude from first positive event following a top-gas reflection event (within a pre-specified vertical displacement range). The left map is obtained from the 3DBD cube and the right from the Super Resolution mapping. The hypothesis is that large amplitude reflects a high confidence base-gas reflector (corresponding to an interface of high to low gas saturation?), whereas low amplitude reflects that the zone below the gas pocket has too high gas saturation to create a significant seismic reflector.

An estimate of the volume of gas filled rock corresponding to the mapped gas pockets can be calculated. The number of voxels between top and base of a pocket is found based on the thickness maps in **Figure** 16, and the total volume is found by multiplying with the volume of each voxel. The area of each voxel is 12.5m×12.5m and the height is 2ms, which can be transformed into meters using the velocity for gas-filled sand within the Utsira formation. Regions with a minimal, constant distance between the two mapped reflectors are not included in the calculations. For the gas pockets marked 1, 2 and 3 in **Figure** 15 the estimated number of voxels are 19598, 4639 and 8612 respectively. The porosity and gas saturation is needed to estimate the actual volume of gas within the gas pockets. This work will continue, to obtain a final estimate of observed gas.

Integration of time-lapse seismic with reservoir flow model
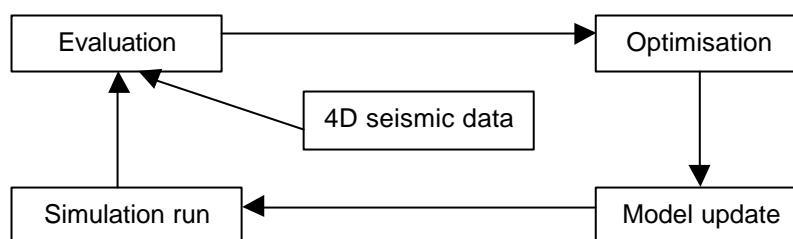Time-lapse data may be compared to results from a simulator with the aim to improve the flow model.

Figure 10 Optimisation loop for matching flow models with 4D seismic.

Subsequent predictions of reservoir behaviour will then be more accurate. Such a "4D seismic history match" is illustrated by the optimisation loop in Figure 10. In this loop time-lapse seismic data is evaluated against results from the flow model. From this evaluation an objective function is constructed as a measure for the difference between the 4D seismic and the flow model. An optimisation algorithm then tries to minimise the objective function by altering a given set of parameters in the model.

In this project it is very important to increase the consistency between the flow model and the 4D seismic. There are large uncertainties in the petro-elastic modelling of the seismic response due to the injected gas. By varying petro-elastic parameters along with the optimisation of the flow model, these parameters may be determined with a greater confidence.

Evaluation of reservoir flow model

To check the consistency between time-lapse seismic and the flow model, a petrophysical model is used. Predicted distributions of saturations and pressures from the simulation are combined with rock properties, using the Gassmann equation, to give the elastic moduli for the seismic model. The parameters are here taken from the 2000 SACS report [1]. The gas has a density of 340 at reservoir conditions, while the bulk modulus is varied in order to span the uncertainty-range of the seismic P-velocity. **Figure** 18 shows the velocity as function of water saturation for different values of the bulk modulus of the gas. From the rock properties and the fluid properties in the flow model, acoustic velocities and impedances are calculated for each grid cell and for each time-step in the model.
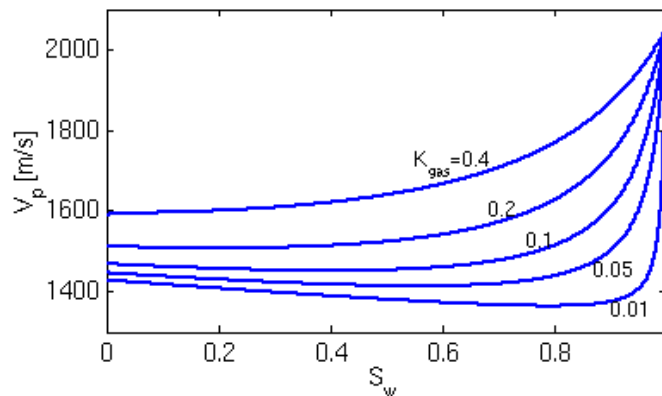

Figure 18 Gassmann-modelled seismic velocity Vp in CO2-water system as function of the water saturation Sw. The density of the gas is 340kg/m3. The bulk modulus of the gas is varied from 0.01 to 0.4 GPa.

Modification in seismic travel time caused by the injected gas can be computed from the synthetically generated velocities. This synthetic pull-down effect predicted from the simulator in 1999 is compared to the corresponding pull-down of the base Utsira in the 1999 seismic in **Figure** 19.
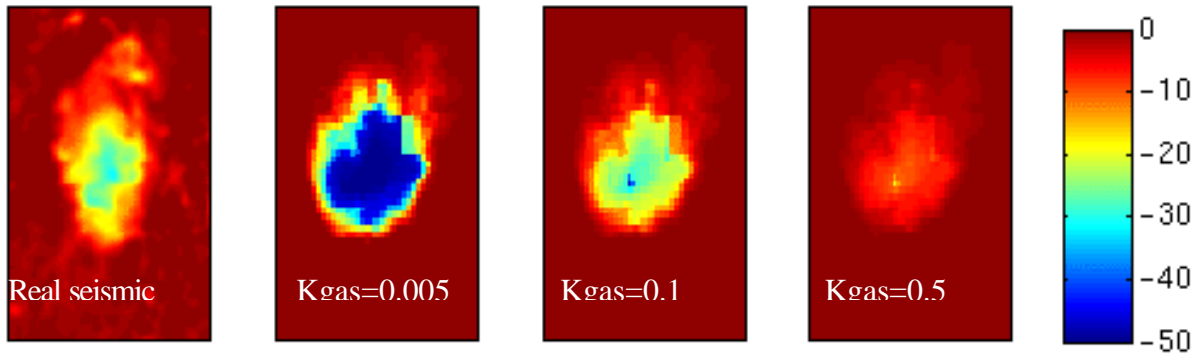
Figure 19 Pull-down of the seismic below the gas cloud in the 1999 seismic (left) and corresponding synthetic pull-down for three different values of the gas bulk modulus (unit GPa).

To quantitatively compare synthetic and real pull-down, a quasi-volume is defined as

$$\int pulldown(x, y) \cdot dx \cdot dy \text{ (unit m}^2\text{s).}$$

Figure 20 shows the observed volume compared to the synthetic volumes for different values of the gas modulus. It is seen that the best match is for $K_{gas} \approx 0.085$. This value of the gas modulus is therefore used in the following calculations. This is slightly larger than 0.0675 which was found to be the most probable value in the 2000 SACS report [1].

The synthetic impedances and velocities are further processed to generate reflectivities and synthetic seismic. This is seen in figure where sections of real and synthetic seismic are compared.
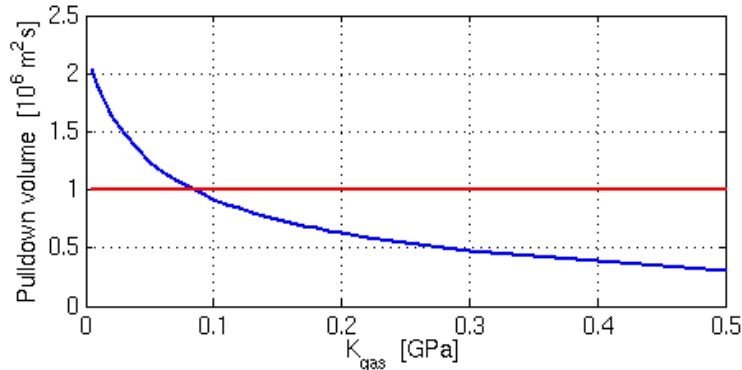

Figure 20 Pull-down volume from the flow model for different values of Kgas (blue line). The red line indicates the volume from real seimic.

Note that the synthetic impedances in the reservoir model have been coupled with the real seismic of the overburden. This has been achieved by a deconvolution of the real seismic. The flow model has nearly horizontal gas layers. It is seen from **Figure** 21 that the synthetic seismic has captured fairly well the depth-to-time distortion of these horizontal reflectors.
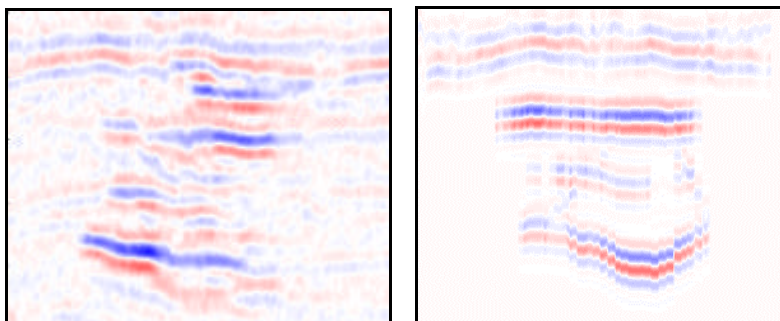

Figure 21 Real and synthetic 1999 seismic.

The flow model (see reference [2]) has four shale layers below top Utsira. These layers are nearly sealing except for a set of highly permeable holes. The basic shape of the layers is the same as the top Utsira formation. In order to update the flow model, the horizontal extension of the different gas layers have been compared. That is, both the depth positions and the thickness of the layers have been ignored. In **Figure** 22 the black regions mapped from the flow model corresponds to Sgas > 0.75. The associated regions from the seismic are also shown in the figure. In mapping the gas from the seismic, a uniform layer thickness of 10 m has been assumed. By considering the non-linearity of the Gassmann curves in **Figure** 18 it is clear that there are inevitably large uncertainties in the estimates of the gas saturation from the seismic. Particularly when the bulk modulus of the gas is low the seismic will not be able to distinguish between different levels of gas-saturated rock.

The most striking difference between the gas observed in the seismic and the gas distribution of the flow model is that the flow model under-predicts the vertical flow of gas. In 1999 the model does not give any gas accumulation below Top Utsira and the shallowest shale layer.

Updating the reservoir flow model
Since gravitational segregation is a dominating physical process in this flow, the positions and size of the holes in the shale layers were optimised in a history match. Also the shape of the shale layer above cloud 3 could be modified. The flow model was coarsened in order to reduce the simulation time. After a set of modifications of the flow model, the gas rose faster to the top of the Utsira sand, and an overall improved match was obtained.

Figure 22 Horizontal extensions (black regions) of the 5 gas clouds in the Utsira sand observed in the 1999 seismic (5 upper images) and the gas (S_{gas} >0.75) below the 5 vertical barriers predicted from the flow model in 1999 (5 lower images). The shaded regions indicate the positions of the high-permeable holes in the shale layers in the flow model.

The history match is planned to continue with an automatic run based on simulated annealing as the optimisation algorithm. Having a final matched model, the consistency check of synthetic and real pull-down will be repeated to verify the petro-elastic model used. The history match will also consider the permeability of the shale layers. The distribution of low consentration CO_2 will have a large impact on the synthetic pull-down volume.

The 4D workstation software development

The 4D Workstation project was initiated with the primary goal of integrating existing 4D functionality and to identify and implement functionality needed for a more streamlined workflow. New functionality has been written using Java and OpenSpirit in order to take advantage of developments in both programming technology and distributed data access. Elements of the 4D workstation is being developed within the SACS2 project. However, in this section the entire workstation is described for completeness.

The Launcher

The need for an integrating launcher resulted in the 4D Workstation application launcher depicted in **Figure**
. It is a one click Java WebStart launcher and, for newer Java-based applications, also offers one click deployment. This means that the user will always have access to the latest version of the software every time the application starts.
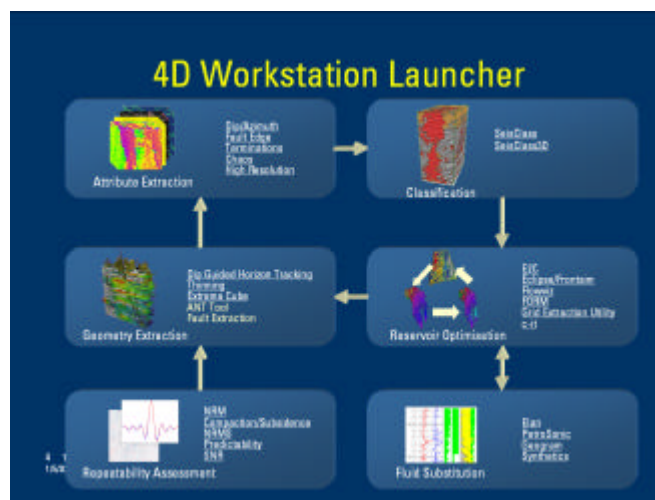

Figure 23 The 4D workstation launcher.

If we examine **Figure** 23 more closely, we see a mix of familiar GeoFrame applications and quite a few new ones. The workflow starts with a Repeatability Assessment phase, and then enters the main reservoir optimisation loop, consisting of geometry extraction, attribute extraction, classification and then reservoir optimisation. As a part of the reservoir optimisation phase, fluid substitution could be performed in order to better understand the seismic response.

Software and data access

In order to make the 4D Workstation software as accessible as possible, we decided to use the Java programming language for all new developments. Not only has Java shown a marked increase in programmer productivity, but programs also tend to have a lot less bugs. In addition to this, Java has a large toolbox available. This makes many tasks trivial that would have required a substantial effort in other programming languages like C++.

When it comes to data access, we choose to implement a simple layer of business objects modelling seismic entities like seismic cubes, horizons and well-logs, in addition to reservoir entities like reservoir simulation grids and flow-lines. This layer was named RAPID (Research API for Development) and has been mapped to several physical databases through the OpenSpirit framework, but also directly to flat files, including Eclipse and FrontSim, and GeoFrame. The RAPID architecture is shown in **Figure** 24. At the bottom of the figure we see the server side with the currently implemented databases, or backends as they are usually called. We see that both GeoFrame and Landmark are available through the commercial

OpenSpirit server. In addition to this, we have made a direct link to GeoFrame, as this is easier to use in an environment where GeoFrame is already installed. We also have a flat file backend that allows a user to mirror any of the other RAPID enabled backends into a file directory and also select for which data entities the bulk data should be downloaded. The user can then, as an example, take these data onto a portable PC and run RAPID-enabled software like if it was against a live database. If data items or bulk data are created/updated, these changes can be transferred back as soon as the user hooks the portable PC back onto the required network. The benefit of a flat file backend when doing developments and debugging, is also self-evident.
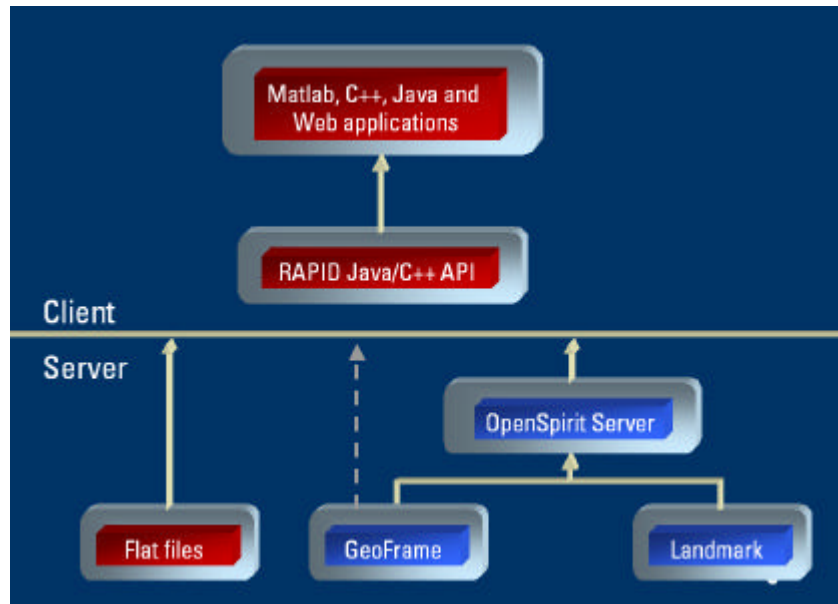

Figure 24 The RAPID architecture.

The client application will get all its data through RAPID, and will in effect don't know (or care for that matter) where the data came from physically. For a developer this provides a nice abstraction, and greatly simplifies coding. RAPID is available in a multi platform Java version, and also as a C++ for both Microsoft Windows and Sun Solaris.

Batch Oriented Processing

The traditional approach to attribute generation has been to compute attributes one by one in a sequential fashion. The user would then monitor the progress in order to be ready to start the next attribute generator. For some of the attributes, it takes hours and even days to compute a seismic cube, and normally something like 20 attributes are computed, so this is clearly and area where throughput should be increased. Hence, there is a significant a need for batch-oriented processing applications. We initially set out to make a multithreaded[3] attribute generator for all of 1D (well-logs), 2D (horizons) and 3D (seismic) data. This computation of attributes, especially for 3D data, is so time consuming that it is not realistic to do this on the fly when the attributes are needed, but rather compute the attributes up front and store them persistently in the database.

---

[3] A multithreaded application can run several tasks at the same time, like running a lengthy processing task in the background while the user still can use the application interactively.

To streamline the attribute generation process, we developed the RAGE (Research Attribute Generation Environment) application as shown in **Figure** 25. In the top left window, the user selects an attribute generator from the tree structure, and this will open a new window in the main work canvas on the right where the user can choose data items and set parameters. The user can also select, and switch, which RAPID backend he wants to work on, so data can be read from all available backends without restarting the application. The figure shows three simple attribute generators, and the status windows below the main work canvas shows the progress of the three attribute generators running simultaneously. On a multiprocessor machine, the processes started in RAGE will spread out evenly on the available processors thanks to the built in load balancing mechanisms of Java.
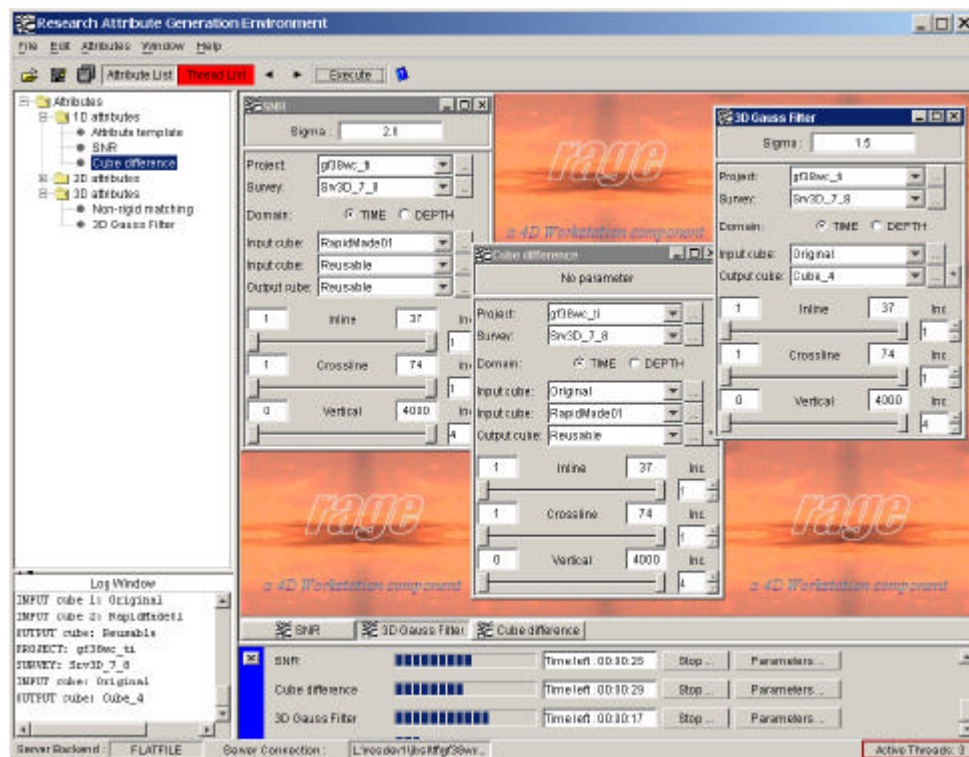

Figure 25 A screenshot of the RAGE user interface.

As the RAGE application framework construction proceeded, we found the architecture to be useful for more applications than we originally though, and we now half jokingly think that RAGE should instead be an acronym for "Research Application Generic Environment". If we look back at **Figure** 23, RAGE now covers applications from the three boxes on the left, feasibility assessment, geometry extraction and attribute extraction.

We have also included 2D viewers for seismic and horizons, so that the user can check the results of a process without having to switch to a visualization application. Future enhancements will include visualization of well logs. It would also make sense to add the 3D viewer, described next, directly into the RAGE framework. Adding to this, we also hope to include a batch queue, and possibly a save option for a set of process parameters in order to facilitate a rerun of the processes.

3D Visualization

Traditional G&G 3D visualization applications have not been able to integrate data entities from both the seismic domain and the reservoir domain. This functionality would be especially useful in a 4D setting where

the user wants to switch back and forth between the two domains during an iterative workflow as the one outlined in **Figure** 23. In order to empower the user with multi domain visualization, we developed a set of visualization framework components called *c-it*. There is one component for each of seismic, horizons, well traces, reservoir model grids and flow-lines. The *c-it* framework is written in Java3D and will as such run on any platform supporting the Java3D runtime, like PC's (Windows and Linux), Sun Workstations or even SGI high end visualization systems. Somewhat surprisingly, we found that the latest generation of PC graphic cards perform very well, and in many cases better than their more expensive workstation counterparts. The big driver here is of course the 3D game playing market. Unfortunately this means that some types of functionality, that would benefit scientific visualization, are lacking, notably 3D textures and stereo viewing capabilities.

Conclusion

It is still early days for the 4D Workstation, but many important applications have already been built, and first steps towards a tighter integration of the various components have been taken. We will continue this work towards our vision of one integrated solution for the whole 4D workflow, giving our users state of the art tools to significantly reduce the effort involved in taking on advanced 4D studies.

References

[1] SACS2: Report from the Geophysics work area, 31.12.00

[2] Sintef

[3] Lindeberg, E., Zweigel, P., Bergmo, P., Ghaderi, A., & Lothe, A.:Prediction of CO2 dispersal pattern improved by geology and reservoir simulation and verified by time lapse seismic. 5th International Conference on Greenhouse Gas Control Technologies, Cairns (Australia), August 2000.